

# Growth of BaMoO<sub>4</sub> and BaCO<sub>3</sub> crystals in silica gel media

S.-A. CHO, J. A. GOMEZ, R. CAMISOTTI, and J. C. OHEP\*

*Department of Metallurgy and Materials Science, Instituto Venezolano de Investigaciones Cientificas (I.V.I.C.), and School of Metallurgical Engineering and Materials Science, Universidad Central de Venezuela, Caracas, Venezuela*

Barium molybdate, BaMoO<sub>4</sub>, and barium carbonate, BaCO<sub>3</sub>, crystals have been grown in sodium metasilicate gels. The influence of concentration of reactant solutions and pH of gels on the nucleation and growth, and on the penetration depth of the growth front of BaMoO<sub>4</sub> crystals in the test tubes were primarily studied. Combinations of pH 6 gel mixture with the 0.4 M and 0.6 M supernatant BaCl<sub>2</sub> and Na<sub>2</sub>MoO<sub>4</sub> solutions resulted in the best size of crystals, inter-crystalline separation and clarity of the gel media. Two best test tube experimental combinations of hybrid growth were repeated in the U-shaped glass tubes to obtain further information. Depending on the growth sites in the tubes, different morphologies of the crystals were observed. The bulk morphologies of these crystals were studied by scanning electron microscopy. Growth of BaCO<sub>3</sub> crystals was performed only as exploratory work in the test tubes.

## 1. Introduction

Although crystallization in gel media was performed as long ago as 1897 and 1914 [1, 2], interest in gel media for crystal growth was not greatly stimulated until recent work of Henisch and co-workers [3, 4]. Although the production of useful crystals through gel media needs further investigation, the possibility of using gel media for the growth of crystals by reaction allows many interesting experimental exploitations of such effects as electrical fields in accelerating and controlling the diffusion of the reactant in gels and across semipermeable membranes, as well as the new opportunities they present for studies on the mechanism of crystal growth processes. It is also advantageous in that the gel method could be used to grow various sorts of crystals — ionic, organic and even metallic crystals — at ambient temperatures [5]. In addition, the apparatus and methods are very simple.

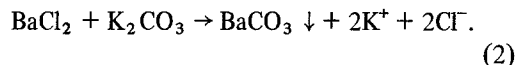
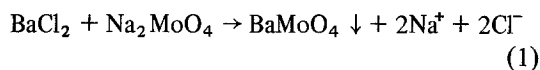
In this report, the influence of concentration of reactants and pH of the gel medium upon aspects of crystallization and bulk morphology of the crystals formed are studied.

\* At Universidad Central de Venezuela only.

## 2. Experimental details

The crystallization apparatus used for the growth of BaMoO<sub>4</sub> consisted of test tubes 16 mm diameter and 10 cm high, and U-shaped glass tubes 20 mm diameter and 14 cm high. For growth of BaCO<sub>3</sub> crystals, a test tube 16 mm diameter and 15 cm high was used.

The chemical reactions taking place in the gel media for the formation of crystals were:



The chemically pure BaCl<sub>2</sub> · 2H<sub>2</sub>O was obtained from Merck AG, Darmstadt and the reagent grade sodium metasilicate (Na<sub>2</sub>SiO<sub>3</sub> · 9H<sub>2</sub>O) was obtained from the Fisher Scientific Company. Other reactants employed in these experiments were reagent grade from Baker Chemical Company.

Silica gels, pH 6, 7 and 8, were prepared by mixing 10 wt% sodium metasilicate water solutions and 3 M acetic acid solution. In order to

determine the best experimental conditions leading to the growth of large and well formed crystals, five reactant solutions of different concentrations, 0.2, 0.4, 0.6, 0.8 and 1.0 M, were prepared. The first experiments were conducted in test tubes. 1.7 ml BaCl<sub>2</sub> solution of each concentration were added to the five 10.0 ml gel solutions of each pH before gelation had occurred; the mixtures were then permitted to gel. Of these, the following combinations of gel pH and BaCl<sub>2</sub> concentration did not form good gel mixtures:

- gels pH = 6, 7 and 8 plus BaCl<sub>2</sub> solutions > 0.8 M
- gels pH = 7 and 8 plus BaCl<sub>2</sub> solutions > 0.6 M
- gel pH = 8 plus BaCl<sub>2</sub> solutions > 0.4 M.

These mixtures resulted in rather hard, cloudy and heterogeneous gels, and because of this, these combinations were eliminated from the experiment. As a consequence, the gel mixtures in the first test tubes experiment consisted of the following combinations of gel pH and BaCl<sub>2</sub> solution concentrations:

Gel pH	BaCl <sub>2</sub> solution concentration (M)
6	0.2, 0.4 and 0.6
7	0.2 and 0.4
8	0.2

For the growth of BaMoO<sub>4</sub> crystals, equal quantities of supernatant Na<sub>2</sub>MoO<sub>4</sub> solutions of equivalent concentrations to the BaCl<sub>2</sub> solution in the gel mixtures, were carefully added to each test tube, the combination of pH 6 gel mixture with 0.4 M and 0.6 M supernatant solutions gave the best results in terms of size of crystals, the separation between the crystals and the clarity of the gel media: this is discussed in the next Section. These two best test tube experimental combinations were repeated in two separate U-tubes, in order to take advantage of hybrid methods (U-tubes, dumb-bell and double diffusion systems) over the simple test tube method [3, 6–8].

The U-tube has the advantage of providing greater freedom for lateral ionic diffusion [7]. Both reactant concentrations are also well defined and reaction point concentrations can be approximated [9]. The advantages of the U-tube method over the test tube method are well explained by Laudise [8] in terms of distribution curves of both ionic concentrations and their product. Because of these advantages, information

on the shape and size of crystals, size distribution and nucleation density, as well as location of the crystallization zone in the tube, can easily be obtained.

Two U-tubes were each filled with 35 ml pH 6 gel solutions. As soon as gelation had occurred, 13 ml each of reactant BaCl<sub>2</sub> and Na<sub>2</sub>MoO<sub>4</sub> solutions were poured onto the gels in each side of the U-tubes; one of the U-tubes was filled with 0.4 M and the other by 0.6 M reactant solutions.

For the growth of BaCO<sub>3</sub> crystals, a combination of 14 ml pH 6 gel mixture containing 5 ml 0.6 M BaCl<sub>2</sub> reactant and an equal quantity of supernatant 0.6 M K<sub>2</sub>CO<sub>3</sub> solution has been studied in a test tube as mentioned before. This experiment was performed merely as an exploratory study in a test tube only for the growth of BaCO<sub>3</sub> crystals.

All SEM photographs were taken using a Hitachi Model MSM-2 scanning electron microscope.

### 3. Crystallization

For the test tube experiments, the nucleation in the gel mixtures BaCO<sub>3</sub> and BaMoO<sub>4</sub> crystals started, in all cases, near the interface of the supernatant solution and the gel mixture about 1 day after addition of the supernatant feed sol-

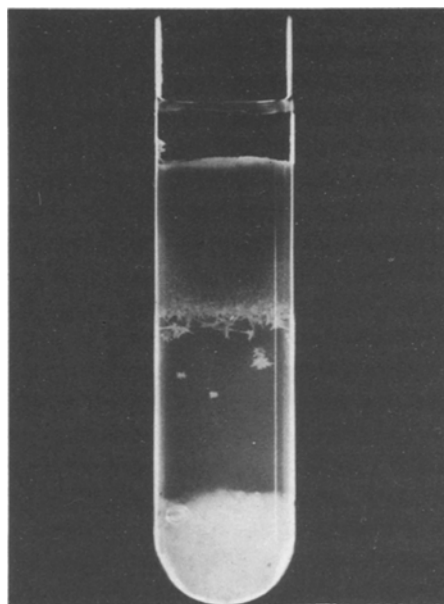


Figure 1 The growth tube for BaCO<sub>3</sub> crystals. Note the two types of crystal; the snow-flake like crystals formed at the upper growth front, and the polycrystalline ball aggregates at the upper interface of the white precipitate at the bottom of the tube.

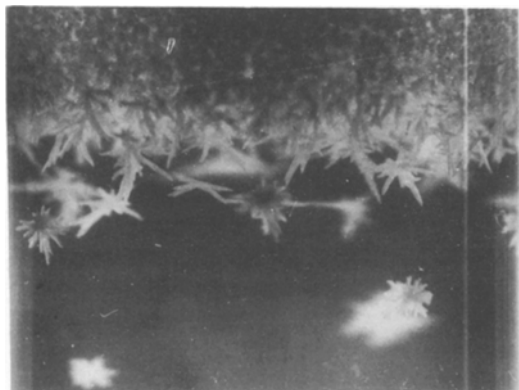


Figure 2 Detailed view of the snow-flake like  $\text{BaCO}_3$  crystals at the growth front in the test tube of Fig. 1.

utions. The growth fronts gradually penetrated down into the gel mixtures with time.

In the case of  $\text{BaCO}_3$ , snow-flake dendritic crystals developed at the growth front. As growth proceeded, white precipitates accumulated at the bottom of the test tube. Towards the end of the experiment, several round polycrystalline balls were observed at the top of the precipitates. The two morphologically different crystals are shown in Fig. 1. Fig. 2 shows an enlarged view of the growth interface (the penetration layer) in the tube. Both photographs were taken just before the crystals were harvested toward the end of the test run about 1 month after the start of the experiment.

For  $\text{BaMoO}_4$ , the overall penetration depth of the crystal growth front, and the nucleation and growth rates (nucleation density and crystal size) were visually examined about 20 days after the onset of the experiment. The general trend in observed magnitudes of these parameters observed for each experimental combination were:

#### penetration depth

pH 6 gel mixture:  $0.2 \text{ M} < 0.6 \text{ M} < 0.4 \text{ M}$  feed solution

pH 7 gel mixture:  $0.2 \text{ M} < 0.4 \text{ M}$  feed solution

0.2 M feed solution:  $\text{pH } 6 < \text{pH } 7 < \text{pH } 8$  gel mixture

0.4 M feed solution:  $\text{pH } 6 < \text{pH } 7$  gel mixture

#### nucleation rate

pH 6 gel mixture:  $0.2 \text{ M} < 0.4 \text{ M} < 0.6 \text{ M}$  feed solution

pH 7 gel mixture:  $0.2 \text{ M} < 0.4 \text{ M}$  feed solution

0.2 M feed solution:  $\text{pH } 6 < \text{pH } 7 < \text{pH } 8$  gel mixture

0.4 M feed solution:  $\text{pH } 6 < \text{pH } 7$  gel mixture

#### growth rate

pH 6 gel mixture:  $0.2 \text{ M} < 0.6 \text{ M} \ll 0.4 \text{ M}$  feed solution

pH 7 gel mixture:  $0.2 \text{ M} < 0.4 \text{ M}$  feed solution

0.2 M feed solution:  $\text{pH } 7 < \text{pH } 8 < \text{pH } 6$  gel mixture

0.4 M feed solution:  $\text{pH } 7 \ll \text{pH } 6$  gel mixture

In terms of clarity of the gel mixture, separation between the crystals and form of the crystals, the combination of pH 6 gel mixture and 0.2 M supernatant feed solution gave the best result. In addition to the above observations, combinations of pH 6 gel mixture plus 0.4 M and 0.6 M feed solutions appeared to be the best for further study in U-tubes, based on the size of crystals produced. In order to obtain more extensive information on the growth behaviour of the crystals, the selected combinations of gel and feed solutions were prepared in two U-tubes. In the U-tubes containing 0.4 M and 0.6 M reactant feed solutions nucleation of  $\text{BaMoO}_4$  crystals began 6 and 5 days respectively, after the feed solutions had been added. The early crystallization sites in the gel media were shifted a little towards the arm containing the  $\text{Na}_2\text{MoO}_4$  solutions. This phenomenon is probably due to the difference in diffusion velocities of the two ions,  $\text{Ba}^{2+}$  and  $\text{MoO}_4^{2-}$ , coming from opposite directions through the gel media, because of the difference in the ionic sizes of the ions.

About 2 weeks later it was observed that the U-tube containing 0.4 M feed solution had a lower nucleation density and better formed, well separated and slightly larger crystals than in the 0.6 M

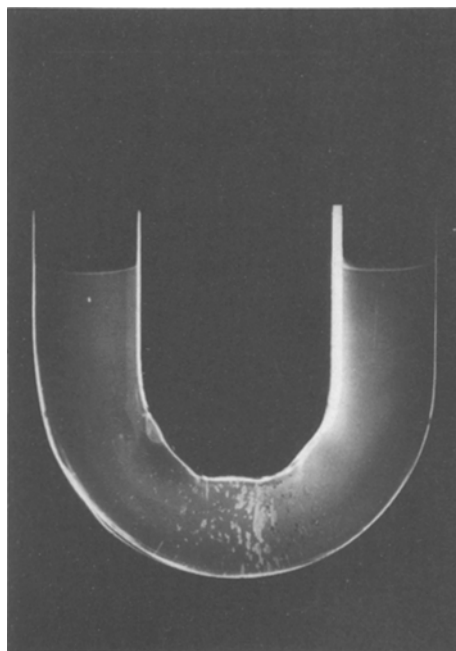


Figure 3  $\text{BaMoO}_4$  crystals grown in the U-tube containing pH 6 silica gel and 0.4 M reactant feed solutions:  $\text{BaCl}_2$  solution is in the left arm and  $\text{Na}_2\text{MoO}_4$  solution is in the right arm.

food solution. Fig. 3 shows the 0.4 M experimental apparatus. The photograph was taken towards the end of the experiment, and the  $\text{BaCl}_2$  and  $\text{Na}_2\text{MoO}_4$  reactant feed solutions are contained in the left- and right-hand arms, respectively.

Towards the end of the crystallization process, the U-tube containing 0.6 M feed solution formed a thin white solid layer near centre of the crystallization had begun. This layer was considered to be a by-product –  $\text{NaCl}$ . The  $\text{NaCl}$  layer is thought to be formed by the supersaturated ions,  $\text{Na}^+$  and  $\text{Cl}^-$ , which have accumulated at this point during the long crystallization process. The absence of an  $\text{NaCl}$  layer in the tube containing 0.4 M feed solutions may be explained by the low concentration of reactants not producing a strong enough ionic saturation at the same stage of the experiment.

The crystals in both U-tubes were harvested 40 days after addition of the feed solutions. All the crystals were cleaned with distilled water and rewashed ultrasonically in a distilled water bath, and then dried naturally in the open air. The crystals were all identified as  $\text{BaCO}_3$  and  $\text{BaMoO}_4$  by X-ray diffraction with Ni filtered  $\text{CuK}\alpha$  radiation.

## 4. Morphology

### 4.1. $\text{BaCO}_3$ crystals

Both types of  $\text{BaCO}_3$  crystal (the snow-flake like dendrites and the round polycrystalline balls), mentioned above were optically translucent and irregular in shape. Fig. 4 shows an SEM view of five pieces of dendrite arms of a snow-flake type dendritic  $\text{BaCO}_3$  crystal. An enlarged SEM view of one is shown in Fig. 5. The dendrite arm has the appearance of a branch and its surface is rough. The crystal does not appear to be well developed

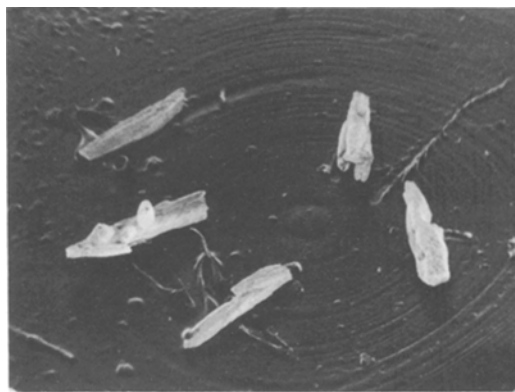


Figure 4 Separated and broken pieces of individual dendrite arms of the snow-flake like  $\text{BaCO}_3$  crystals,  $\times 30$ .

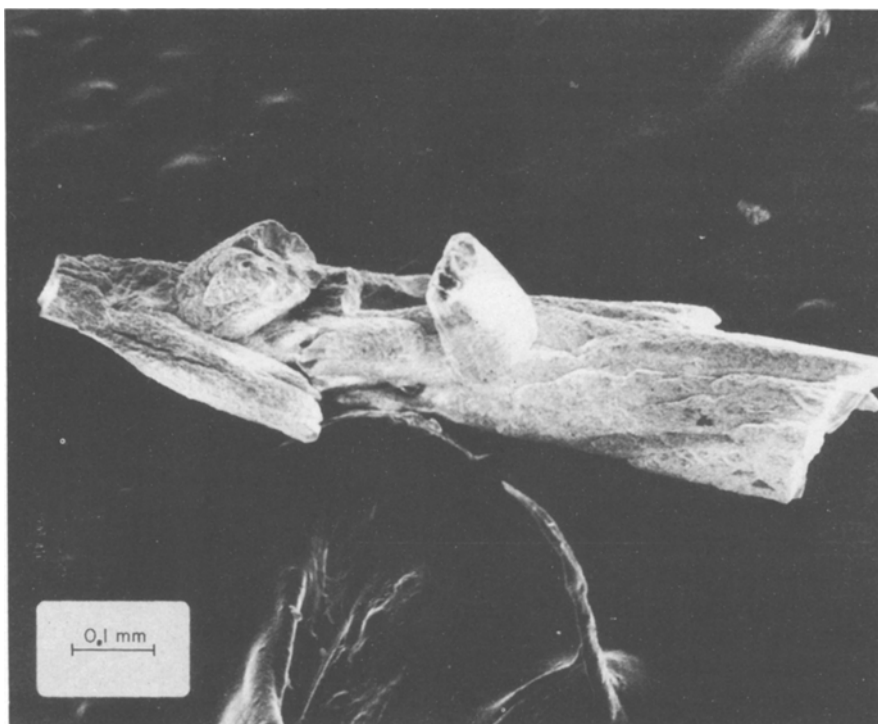


Figure 5 An SEM of one of the dendrite arms of the snow-flake like  $\text{BaCO}_3$  crystals seen in Fig. 4. The crystal has the appearance of a branch of a tree. Note the irregular shape and rough surface.

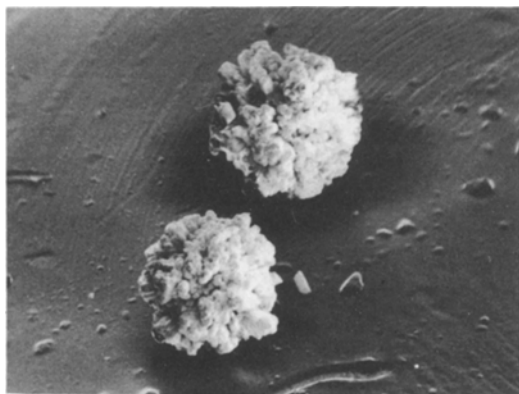


Figure 6 SEM of the round polycrystalline ball aggregates of  $\text{BaCO}_3$  crystals,  $\times 30$ .

but seems to be formed as various layers of crystallites. The overall morphology of the crystal is rather poor in terms of the well developed geometrical crystalline state. The surface morphology shown in Fig. 5 looks like very old bones. Fig. 6 shows the round polycrystalline aggregate

$\text{BaCO}_3$  balls. The bulk surface morphology of these is similar to that of sea coral.

#### 4.2. $\text{BaMoO}_4$ crystals

The morphology of the  $\text{BaMoO}_4$  crystals in the U-tubes could be divided into three groups depending on the crystallization zones where they formed in the tubes. The three zones, shown in Fig. 3, are the left-hand side zone in the arm containing the  $\text{BaCl}_2$  reactant solution, the central zone at the position where early crystallization started, and the right-hand side zone in the arm containing the  $\text{Na}_2\text{MoO}_4$  reactant solution. Figs. 7a to d show four typically different shapes of  $\text{BaMoO}_4$  crystals. These crystals formed in the left-hand side crystallization zone. They were columnar in shape and could form single needles (Fig. 7a and b), cruciforms (Fig. 7c) and starlike dendrites (Fig. 7d). The needle and cruciform shapes (Fig. 7a to 7c) were formed at distances respectively further from the central crystallization zone towards the U-tube arm containing the

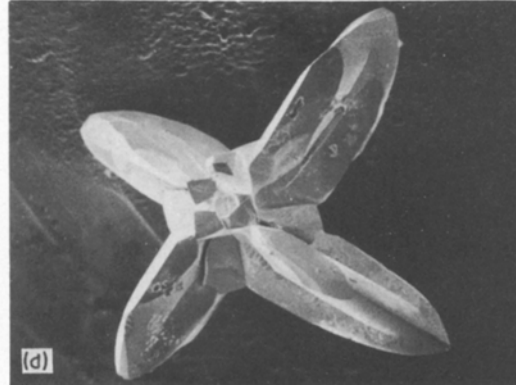
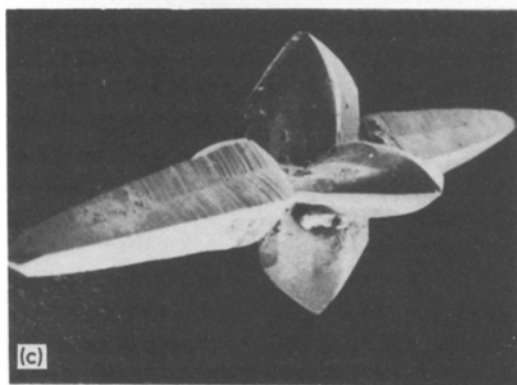
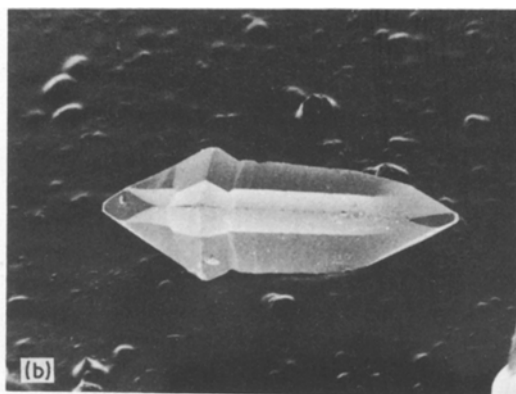
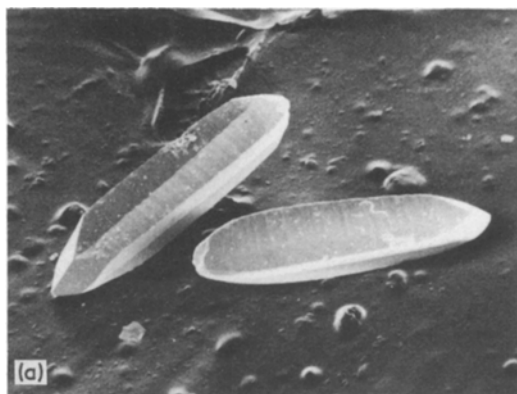
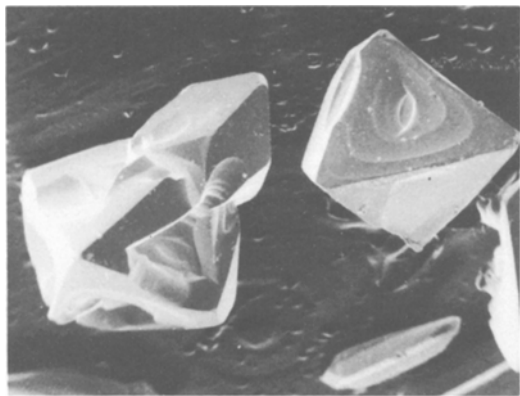


Figure 7 SEMs of (a) needle-like  $\text{BaMoO}_4$  crystals,  $\times 50$ ; (b) half developed semicruciform  $\text{BaMoO}_4$  crystals,  $\times 50$ ; (c) fully developed cruciform  $\text{BaMoO}_4$  crystals,  $\times 50$ , note the tidal marks on the two longest needles; and (d) well developed star-like  $\text{BaMoO}_4$  dendrite crystals,  $\times 50$ . This group of crystals was formed in the left-hand side crystallization zone in the U-tube arm containing  $\text{BaCl}_2$  solution.



*Figure 8* SEM of the bulky octahedral BaMoO<sub>4</sub> crystals formed in the central crystallization zone of the U-tube,  $\times 30$ . Note the surface defects and twins.

BaCl<sub>2</sub> solution. The well-developed star-like dendritic crystals (Fig. 7d) formed very close to the central crystallization zone where the well-shaped bulky octahedra and their morphologically related crystals shown in Fig. 8 were predominant. The last group of crystals formed in the right-hand side crystallization zone, and appeared to be aggregates of small crystallites. These crystals are typically round polycrystalline balls, and look like the round BaCO<sub>3</sub> polycrystalline balls shown in Fig. 6. The balls were not transparent like the rest of the crystals but were optically translucent.

Figs. 7c and 8 shows surface irregularities on some crystal facets in addition to the twins seen in Fig. 8. The two longest needle arms of the curciform dendrite of Fig. 7c have growth striae (tidal marks) on the facets. The origin of these marks is still in question; they may be due either to the temperature fluctuation of the ambient or to vibration of the laboratory bench during the period of the experiment. However, it is interesting to note that the marks only appeared on the two longest dendritic needles while the surfaces of other four short dendrite columns were smooth. On the other hand, crystals very similar to those shown in Fig. 7c, also exhibited tidal marks, but others, even the longest ones, did not. Because of this the marks are considered to be related to the growth orientation against the on-coming direction of the reactants in the gel medium. The origin of the marks may thus be due to the fluctuation in concentration of the reactants occurring due to either the temperature fluctuation or the vibration, or both. However, the definitive reason for the marks is still in question. The conical surface defect on the octahedral crystals seen in Fig.

8 is indented inward. This indentation of the defect may be due to an unbalanced supply of incoming ions diffusing through the gel medium into the growing flat interface of the crystal.

The four small dark facets in the centre of Fig. 7d are the surfaces of small broken dendrite arms. These reveal that the arms are not well formed but are irregular in shape. Fig. 7d also shows how the crystals are contaminated by gel, seen here as small solid pieces stuck to the crystal surfaces. These dried-up gel pieces are also seen on the crystal surfaces in Fig. 7c. It is important that all crystals are cleaned and ultrasonically washed, as described above, before a quantitative study of contamination by a third ion of crystals grown in a gel medium is carried out. This is to ensure that the ion content chemically analysed is due only to the impurity ion absorbed into the crystal and not the gel adhering to the crystal surface. This is checked by high magnification microscopic examination, e.g. SEM.

Fig. 9 shows an enlarged SEM of the tip of one of the needle-shaped crystals in Fig. 7a. One facet is very rough compared to the other three in the photo, indicating that the roughness of the growth interfaces of crystals grown in a gel medium is not even. The reason for this heterogeneity in the degree of roughness among similar growth facets is not as yet clear.

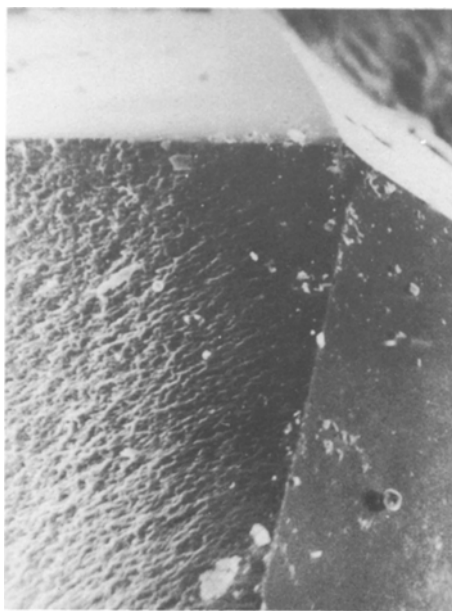


*Figure 9* Enlarged SEM view of the tip of one of the needle-like crystals of Fig. 7a. The roughness of one facet is very different from that of the other facets,  $\times 400$ .

## Acknowledgement

S.-A. Cho is indebted to Professor H.K. Henisch for introducing him to this subject and technique. The authors wish to thank Mr Okada of the Hitachi Corp., for his assistance in taking the SEM photographs.

## References

1. W. OSTWALD, *Z. Phys. Chem.* **27** (1897) 365.
2. R. E. LIESEGANG, *Z. Phys. Chem. (Leipzig)* **88** (1914) 1.
3. H. K. HENISCH, J. DENNIS and J. I. HANOKA, *J. Phys. Chem. Solids* **26** (1965) 493.
4. H. K. HENISCH, "Crystal Growth in Gels" (The Pennsylvania State University Press, University Park, Pennsylvania, 1970).
5. C. BARTA and J. ZEMLIKA, *J. Crystal Growth* **10** (1971) 158.
6. A. F. ARMINGTON and J. J. O'CONNOR, *ibid* **3, 4** (1968) 367.
7. A. R. PATEL and H. L. BHAT, *ibid* **12** (1972) 288.
8. R. A. LAUDISE, "The Growth of Single Crystals" (Prentice-Hall, Englewood Cliffs, New Jersey, 1970) p. 271.
9. J. M. MCCAULEY and RUSTUM ROY, *Amer. Mineral.* **59** (1954) 947.

Received 23 March and accepted 27 July 1976.